Controlled activation of morphogenesis to generate a functional human microvasculature in a synthetic matrix

Donny Hanjaya-Putra,[1] Vivek Bose,[1] Yu-I Shen,[1] Jane Yee,[1] Sudhir Khetan,[2] Karen Fox-Talbot,[3] Charles Steenbergen,[3] Jason A. Burdick,[2] and Sharon Gerecht[1]

[1]Department of Chemical and Biomolecular Engineering, Johns Hopkins Physical Sciences-Oncology Center and Institute for NanoBioTechnology, Johns Hopkins University, Baltimore, MD; [2]Department of Bioengineering, University of Pennsylvania, Philadelphia, PA; and [3]Pathology, Johns Hopkins University School of Medicine, Baltimore, MD

Understanding the role of the extracellular matrix (ECM) in vascular morphogenesis has been possible using natural ECMs as in vitro models to study the underlying molecular mechanisms. However, little is known about vascular morphogenesis in synthetic matrices where properties can be tuned toward both the basic understanding of tubulogenesis in modular environments and as a clinically relevant alternative to natural materials for regenerative medicine. We investigated synthetic, tunable hyaluronic acid (HA) hydrogels and determined both the adhesion and degradation parameters that enable human endothelial colony-forming cells (ECFCs) to form efficient vascular networks. Entrapped ECFCs underwent tubulogenesis dependent on the cellular interactions with the HA hydrogel during each stage of vascular morphogenesis. Vacuole and lumen formed through integrins $\alpha_5\beta_1$ and $\alpha_V\beta_3$, while branching and sprouting were enabled by HA hydrogel degradation. Vascular networks formed within HA hydrogels containing ECFCs anastomosed with the host's circulation and supported blood flow in the hydrogel after transplantation. Collectively, we show that the signaling pathways of vascular morphogenesis of ECFCs can be precisely regulated in a synthetic matrix, resulting in a functional microvasculature useful for the study of 3-dimensional vascular biology and toward a range of vascular disorders and approaches in tissue regeneration. (*Blood*. 2011;118(3):804-815)

Introduction

Generating a functional vascular network can potentially improve treatment for vascular disease and successful organ transplantation.[1] Since their discovery, marrow-derived circulating endothelial progenitor cells (EPCs) have been demonstrated to participate in postnatal vasculogenesis.[2,3] Putative EPCs have been proposed as a potential therapeutic tool for treating vascular disease, either through infusion to the site of vascularization[4-6] or via ex vivo expansion to engineer vascularized tissue constructs.[7-9] Research has shown that endothelial colony-forming cells (ECFCs), a subtype of EPCs recently identified from circulating adult and human umbilical cord blood, express characteristics of putative EPCs.[10,11] These ECFCs are characterized by robust proliferative potential in forming secondary and tertiary colonies, as well as de novo blood vessel formation in vivo.

The complex processes of vascular regeneration and repair require EPCs to break down the extracellular matrix (ECM), migrate, differentiate, and undergo tubulogenesis. In the last decade, our understanding of the role of the ECM in vascular morphogenesis has greatly expanded because of well-defined in vitro angiogenesis models. Such natural ECMs as matrigel, collagen, and fibrin gels have allowed us to study the molecular mechanisms that regulate endothelial cell (EC) tubulogenesis,[12,13] as well as to transplant vascular progenitor cells, such as human embryonic stem (hES) cell–derived ECs,[14] ECFCs,[15] EPCs, and mesenchymal stem cells (MSCs),[8,9,16] to generate vascular networks and in vivo. However, the inherent chemical and physical properties of these natural materials have limited their manipulability for engineering vascularized tissue constructs. Moreover, problems associated with complex purification processes, pathogen transfer, and immunogenicity have hampered their clinical usage.[17] Some have suggested synthetic biomaterials, xeno-free and more clinically relevant for regenerative medicine, as an alternative.[18] Unlike natural ECMs, we can engineer these synthetic biomaterials to provide instructive microenvironments capable of recapitulating complex stages of vascular morphogenesis.[17] Although several studies have attempted to generate vascular network assembly within such synthetic biomaterials in vitro,[19,20] no report to date demonstrates highly controlled vascular morphogenesis in a synthetic material with the potential for in vivo implantation.

Hyaluronic acid (HA; hyaluronan) plays a crucial role in regulating angiogenesis by stimulating cytokine secretion and EC proliferation.[21,22] HA can be processed into well-defined synthetic networks (ie, hydrogels) which not only have high water content, which promotes cell viability, but also biophysical and biochemical properties similar to many soft tissues.[23] HA hydrogels have been used to control the differentiation of hES cells[24] and to probe the various properties that support in vitro vascular morphogenesis.[25,26] Moreover, HA hydrogels are biocompatible, can be designed with a range of mechanical properties, and can degrade along the polymer backbone via hyaluronidases or through peptide crosslinkers susceptible to matrix metalloproteinases (MMPs).[27] Overall, their

Submitted December 23, 2010; accepted April 22, 2011. Prepublished online as *Blood* First Edition paper, April 28, 2011; DOI 10.1182/blood-2010-12-327338.

An Inside *Blood* analysis of this article appears at the front of this issue.

The online version of this article contains a data supplement.

The publication costs of this article were defrayed in part by page charge payment. Therefore, and solely to indicate this fact, this article is hereby marked "advertisement" in accordance with 18 USC section 1734.

biologic relevance, synthetic versatility, and cytocompatibility make HA hydrogels highly useful for studying vascular morphogenesis in a biomimetic environment and in translational therapeutics.

Here, we report the matrix cues required for the sequential activation of morphogenesis to generate a modular vascular construct in a synthetic biomaterial. We exploit the modifiability of the HA hydrogel system and generate a functional human microvasculature from ECFCs that has obvious translation potential for regenerative medicine.

Methods

Human ECFCs

Human umbilical cord blood ECFCs isolated from outgrowth clones, kindly provided by Dr Mervin C. Yoder (Indiana University School of Medicine), were expanded in endothelial growth media (EGM; PromoCell) and used for experiments between passages 6 and 8, as previously described.[11,25,26]

Synthesis of AHA hydrogels

AHA hydrogels were prepared as was previously reported.[27] Briefly, we synthesized AHA using a 2-step protocol: (1) we synthesized the tetrabutylammonium salt of HA (HA-TBA) by reacting sodium hyaluronate (64 kDa; Lifecore Biomedical) with the highly acidic ion exchange resin Dowex-100 and neutralizing with 0.2M TBA-OH; (2) we coupled acrylic acid (2.5/equivalent [Eq]) and HA-TBA (1 Eq, repeat unit) in the presence of dimethylaminopyridine (DMAP; 0.075 Eq) and di-tert-butyl dicarbonate (1.5 Eq) in DMSO, followed by dialysis and lyophilization; we used the ^{1}H NMR spectrum to confirm the final percent modification of the AHA.

Peptides

From GenScript Corporation, we obtained the cell-adhesive peptide GCGYGRGDSPG (molecular weight [MW]: 1025.1 Da; RGDS indicates the RGD integrin-binding domain), cell-nonadhesive peptide GCGYGRDGSPG (MW: 1025.1 Da; RDGS indicates the RDG mutated integrin-binding domain), MMP-sensitive peptide crosslinker GCRDGPQG↓IWGQDRCG (MW: 1754.0 Da; down arrow indicates the site of proteolytic cleavage), and MMP-insensitive peptide crosslinker GCRDGDQGIAGFDRCG (MW: 1754.0 Da), all with > 95% purity (per manufacturer HPLC analysis).

ECFC encapsulation and culture

AHA polymer (3 weight percent [wt%]) was dissolved in a triethanolamine-buffered saline (TEOA buffer: 0.2M TEOA, 0.3M total osmolarity, pH 8.0). The cell-adhesive peptides (RGDS; GenScript) were dissolved in TEOA buffer and added to the AHA solution at final peptide concentrations of 0.37mM, 3.7mM, and 14.8mM (corresponding to 1%, 10%, and 20% of available acrylate groups within 3 wt% AHA) and allowed to react for 1 hour with gentle shaking. Recombinant human $VEGF_{165}$ (Pierce), bFGF (Invitrogen), Ang-1 (R&D Systems), TNF-α (R&D Systems), and stromal cell-derived factor-1 (SDF-1; R&D Systems) were added at 50 ng/mL into the AHA-RGDS mixture. Human umbilical cord blood ECFCs were encapsulated in HA hydrogels with densities of 5×10^6 cells/mL. After the resuspension of cells into this solution, MMP peptide crosslinker (MMP; GenScript) dissolved in TEOA buffer was added at 4.83mM (corresponding to the 25% of available acrylate groups within 3 wt% AHA). Immediately after adding the MMP crosslinker, we pipetted 50 μL of this mixture into sterile molds (5 mm diameter, 2 mm height), and allowed them to react for 15 minutes at room temperature inside the laminar flow hood. The formed constructs were cultured for up to 3 days in EGM (PromoCell). Visualization and image acquisition were performed using an inverted light microscope (Olympus IX50) and a confocal microscope (LSM 510 Meta; Carl Zeiss) at various time intervals along the culture period.

siRNA transfection

ECFCs were transfected with siGENOME SMARTpool human MT1-MMP, Hyal-2, and Hyal-3 (Dharmacon) using the manufacturer's protocol, analyzed with RT-PCR and Western blot, and used as we previously described[25] (supplemental Figure 1, available on the *Blood* Web site; see the Supplemental Materials link at the top of the online article).

Viscoelasticity measurement

We measured oscillatory shear of the elastic modulus (G′) using a constant strain rheometer with steel cone-plate geometry (25 mm in diameter; RFS3; TA Instruments), as previously described.[25,26,28] Briefly, we performed oscillatory time sweeps on 3 samples (n = 3) for each hydrogel group at various time intervals along the culture period. The strain was maintained at 20% during the time sweeps by adjusting the stress amplitude at a frequency of 1 Hz. This strain and frequency were chosen because G′ was roughly frequency-independent within the linear viscoelastic regime. The tests occurred in a humidified chamber at a constant temperature (25°C) in 30-second intervals. The Young modulus (substrate viscoelasticity) was calculated by $E = 2G'(1 + \nu)$. Acrylated HA hydrogels are assumed to be incompressible[23,25,26] such that their Poisson ratios (ν) approach 0.5 and the relationship becomes $E = 3G'$.[28]

VEGF release and degradation study

At various time points, 1 mL of conditioned media from gels alone and from gels containing cells were collected and replaced with fresh growth media. At the final time point (day 3), the gels were degraded using endogenous 1000 IU/mL hyaluronidase IV (Sigma-Aldrich). After 24 hours, we completely degraded the gels and collected the conditioned media. We stored all samples (n = 3) at −80°C before performing an ELISA analysis for VEGF and uronic acid assay. VEGF release profiles were obtained using an ELISA kit (Pierce Biotechnology) following the manufacturer's instructions and as reported in our previous publications. Results are presented in terms of cumulative release as a function of time. To study the degradation kinetics of the gels by the cells, we also analyzed the conditioned media via a modified uronic acid assay, as previously reported.

Vacuole visualization, integrin blocking, and MMP inhibition via TIMP

Quantification of vacuoles and lumen formation was performed following a previous reported protocol.[29] For each condition, we analyzed 200 cells for vacuole and lumen formation. A cell was considered to be vacuolating if > 30% of the cell's area contained a vacuole or lumen. For further visualization using confocal microscopy, we performed FM-464 vacuole staining (Invitrogen) following the manufacturer's protocol. To determine the integrins involved, various Abs directed toward human integrin subunits and heterodimers were added. Inhibition via TIMP-1, TIMP-2, or TIMP-3 was performed as previously described with GM6001 (5μM; Calbiochem) as a negative control.[30] Supplemental Table 1 lists the concentration of each Ab and recombinant proteins used.

Immunofluorescence

We fixed human umbilical cord blood ECFCs cultured in flasks, or encapsulated ECFCs cultured within HA hydrogels, using formalin-free fixative (Accustain; Sigma-Aldrich) for 20 minutes, and washed them with PBS. For staining, cells were permeabilized with a solution of 0.1% Triton-X for 10 minutes, washed with PBS and incubated for 1 hour with primary Ab (supplemental Table 1), rinsed twice with PBS, and incubated with appropriate FITC or Cy3 secondary Abs (1:50; Sigma-Aldrich). After rinsing twice with PBS, cells were incubated with either FITC-conjugated lectin (1:40; Vector Laboratories) or FITC or Cy3-conjugated phalloidin (1:40; Molecular Probes) for 1 hour, rinsed with PBS, and incubated with DAPI (1:1000; Roche Diagnostics) for an additional 10 minutes. The immunolabeled cells were examined using confocal microscopy (LSM 510 Meta; Carl Zeiss).

Transmission electron microscopy

At various time points throughout vascular morphogenesis, the ECFCs and HA-hydrogel constructs (n = 3 for each time point) were prepared for transmission electron microscopy (TEM) analysis. Briefly, the constructs were fixed with 3.0% formaldehyde, 1.5% glutaraldehyde in 0.1M Na cacodylate, 5mM Ca^{2+}, and 2.5% sucrose at room temperature for 1 hour and washed 3 times in 0.1M cacodylate/2.5% sucrose (pH 7.4) for 15 minutes each. The cells were postfixed with Palade OsO_4 on ice for 1 hour, rinsed with Kellenberger uranyl acetate, and then processed conventionally through Epon embedding. Serial sections were cut, mounted onto copper grids, and viewed using a Phillips EM 410 transmission electron microscope (FEI). Images were captured with an FEI Eagle 2K camera.

Scanning electron microscopy

We studied the ultrastructure of the hydrogels using scanning electron microscopy (FEI Quanta ESEM 200). In the case of cell visualization, constructs were fixed as described in "Transmission electron microscopy", postfixed with Palade OsO_4 on ice for 1 hour, then processed as previously described. Briefly, the hydrogels were swelled in PBS for 24 hours, quickly frozen in liquid nitrogen, and then freeze-dried in a Virtis Freeze Dryer under vacuum at −50°C for 3 days, until the samples became completely dry. The freeze-dried hydrogels were fractured to reveal their interior, mounted onto aluminum stubs with double-sided carbon tape, and sputter-coated (Anatech Hummer 6.2 Sputter Coater; Anatech) with Ag for 1 minute. We examined the interior morphology of the hydrogels using scanning electron microscopy at 25 kV and 12 nA.

Real-time RT-PCR

Two-step RT-PCR was performed for *MT1-MMP*, *Hyal-2*, *Hyal-3*, *ITGA2*, *ITGA5*, *ITGAV*, *ITGB1*, *ITGB3*, *TIMP-1*, *TIMP-2*, *TIMP-3*, *Fn*, *HPRT1*, and *β-ACTIN*, and samples were examined in triplicate, analyzed, and graphed (n = 3) as we previously described.[25,26]

Transplantation of vascularized constructs

Vascularized constructs were implanted into the flanks of 6- to 8-week-old nude mice following well-established protocols. Briefly, vascularized constructs and HA constructs alone were cultured in vitro for 3 days and implanted into each flank (left or right, 2 constructs per mouse). Eight to 10 constructs were implanted for each group (n = 8-10). After 2 weeks, we euthanized the mice, harvested the constructs, fixed them in formalin-free Accustain fixative (Sigma-Aldrich), and proceeded to process them histologically. The Johns Hopkins University Institutional Animal Care and Use Committee approved all animal protocols.

Histology

Construct explants were fixed using formalin-free fixative (Accustain; Sigma-Aldrich). This fixative was chosen as it preserves both hydrogel structure and endothelial cell immunoreactivity and morphology compared with commonly used formalin-based fixatives[31] (supplemental Figure 2A), though this alcohol-based fixative causes swelling of RBCs as can be seen in the vasculature in the surrounding tissues and within the gel (supplemental Figure 2A). Attempts to use a zinc-based fixative, which was previously shown to preserve endothelial cell immunoreactivity and morphology[31] failed to preserve the structure of the swollen hydrogel (supplemental Figure 2C-D). After fixation of construct explants, samples were dehydrated in graded ethanol (70%-100%), embedded in paraffin, serially sectioned using a microtome (5 μm), and stained with either H&E or immunohistochemistry for anti–mouse PECAM1, F4/80 and α-SMA or anti–human CD31 (DAKO). Appropriate IgG isotype was used as controls (shown in supplemental Figure 2E). Human blood vessel number and size were counted, measured, and normalized to tissue area. We sampled a minimum of 6 images for each construct, and counted, measured, and normalized the blood vessels accordingly.

Statistical analysis

Expression data of integrins, MMPs, TIMPs, and hyaluronidases were performed on triplicate samples with duplicate readings. We performed VEGF and uronic acid release on triplicate samples with duplicate readings. Statistical analysis was performed using GraphPad Prism 4.02 (GraphPad Software Inc). *t* tests were performed to determine significance using GraphPad Prism 4.02. Significance levels were determined using posttests, and were set at $*P < .05$, $**P < .01$, and $***P < .001$. No significant difference ($P > .05$) was indicated by #. All graphical data were reported.

Results

HA hydrogels

We hypothesized that HA hydrogels formed from acrylated HA (AHA) precursors can provide the dynamic cues required for network assembly of encapsulated ECFCs (Figure 1). These hydrogels, formed from AHA molecules, can first be modified with integrin-binding adhesive peptides (via conjugate addition reactions between thiol groups on RGDS-containing peptides and acrylates along the HA backbone), and then crosslinked with dithiol peptide crosslinkers (thiol groups on each end of peptide react with acrylates).[27] These hydrogels use an enzymatically degradable peptide (with sequence GCRDGPQG ↓ IWGQDRCG susceptible to both MMP-1 and MMP-2[32,33]) as the crosslinker. The AHA in this study, ~ 50% modified (50% of the repeating groups on the HA macromer contain acrylates), was used to form 3 wt% hydrogels (supplemental Figure 3A-B). Pilot studies determined these parameters to be optimal for cytocompatibility and vascular morphogenesis (supplemental Table 2). In addition, several soluble factors—namely VEGF, bFGF, and angiopoietin 1 (Ang1) that are needed for vasculogenesis, as the literature has extensively established[12,34,35]—were incorporated with the hydrogels. In addition, stromal cell-derived factor-1 (SDF-1) and TNF-α are known to induce MMP production in ECs,[36] which need an optimum MMP secretion to allow vascular branching and network formation.[37,38] Therefore, we also encapsulated SDF-1 and TNF-α to promote cell sprouting and invasion.[33,39] We used each of these factors in all described studies; thus, this work focused on alterations in the matrix components.

Matrix considerations for vascular morphogenesis: adhesion and degradation

As our first step in designing a modular vascular hydrogel system, we determined whether the adhesion sites within AHA hydrogels promote the formation of vacuoles that subsequently coalesce into open lumens in ECFCs. We varied concentrations of RGD peptide within AHA hydrogels to determine the dose-dependence of tubulogenesis on adhesivity. Based on previous reports examining the role of RGD adhesion in tubulogenesis in fibrin gels,[29] we generated HA hydrogels with RGD concentrations of 0.37mM, 3.7mM, and 14.8mM and analyzed the kinetics of vacuole and lumen formation. We found that vacuole and lumen formation is RGD dose-dependent and that the optimal RGD concentration in our system is 3.7mM, corresponding to ~ 10% of acrylate consumption (Figure 2A; supplemental Figure 3C). We detected very little vacuole formation with no lumen formation in hydrogels generated with 0.37mM RGD concentration, while higher concentrations of RGD did not significantly enhance vacuole formation. We observed little or no vacuole and lumen formation when using the mutated adhesion site RDG. We then examined the necessity of MMP-sensitive crosslinker incorporation into the HA hydrogels

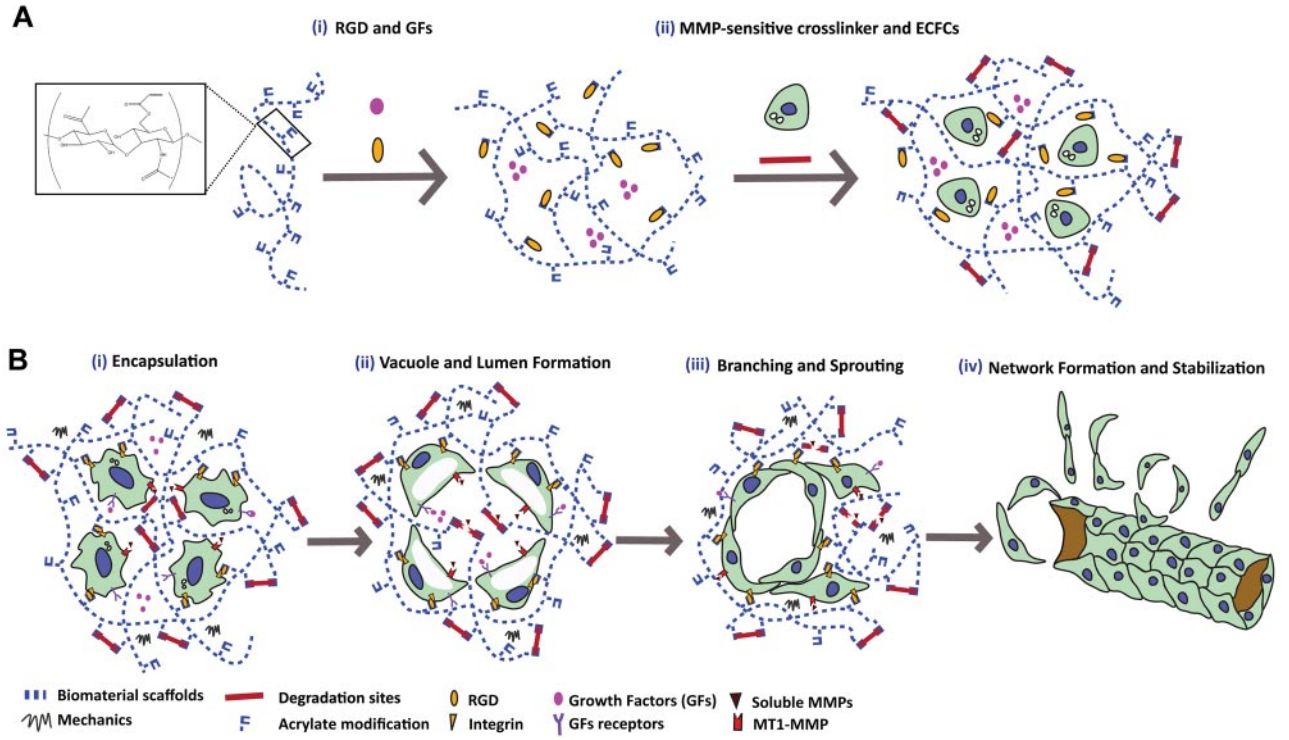

Figure 1. HA-hydrogel synthesis and study strategy. (A) Schematic of AHA hydrogels. AHA hydrogels are formed by reacting AHA molecules with RGD-containing peptides and encapsulating soluble growth factors (GFs; i). ECFCs and MMP-sensitive crosslinkers are then added to form the constructs (ii). (B) Schematic of vascular morphogenesis activation strategy at each stage during culture of AHA hydrogels. In response to RGD and soluble GFs, encapsulated ECFCs undergo vacuole formation, the first initial step in vascular morphogenesis. Vacuolated ECFCs then merge with the neighboring cells to form an open lumen compartment (i-ii). MMP-sensitive crosslinkers subsequently enable ECFC tubulogenesis to progress through both branching and sprouting, to form complex and comprehensive vascular networks (iii-iv).

(Figure 2B; supplemental Figure 3D). We previously demonstrated that hydrogels with moderate viscoelasticity supported 2-dimensional ECFC morphogenesis.[25] We therefore examined a range of MMP-sensitive crosslinker concentrations, corresponding to 10% to 50% acrylate consumption,[27] and found that ~ 25% (4.83mM) supported rapid network formation while sustaining hydrogel integrity throughout the morphogenesis (data not shown). When RDG and an MMP-insensitive crosslinker were used, no vacuole or lumen was observed. However, when using RGD and an MMP-insensitive crosslinker, we observed vacuoles but with networks of limited extent. These results show that RGD regulates vacuole and lumen formation within synthetic HA hydrogels in a dose-dependent manner and that an MMP-sensitive peptide is required to enable the migration of ECFCs to their nearest neighbor to further coalesce into a complex network structures.

Vascular network assembly of ECFCs within HA gels

Day 0-1: Encapsulation and morphogenesis. We sought to determine the morphogenesis dynamics of ECFCs encapsulated within the gels. Throughout the RGD and MMP experiments described above, we observed that vacuole formation completed within 48 hours of encapsulation. We therefore analyzed, in detail, the progression of ECFC morphogenesis within the HA hydrogels. Vacuoles could be observed within 3 to 6 hours after cell encapsulation (Figure 3A). This process continued with vacuoles increasing in number and size, followed by their coalescence into larger lumens at day 1 (Figure 3B).

Day 2: Branching and sprouting. On day 2 of culture, we could observe the progression of ECFC tubulogenesis through both branching and sprouting. We also observed hydrogel degradation in the cell microenvironment alongside cell elongation, potentially suggesting events of guidance channels forming between neighboring cells (Figure 3C).

Day 3: Network formation and growth. By day 3, vascular networks grew; we clearly observed complex and comprehensive structures within AHA hydrogels (Figure 4A). Complex vascular networks with patent lumen structures were easily detected throughout the hydrogels, suggesting a mature vascular network (Figure 4B-D; supplemental Figure 4).

Cell and material interactions: molecular regulation of vascular morphogenesis through adhesion in AHA gels

To determine the integrin subunit that regulates vacuole and lumen formation within these synthetic AHA hydrogels, we performed an integrin-blocking experiment. We tested 3 integrins—$\alpha_v\beta_3$, $\alpha_5\beta_1$, $\alpha_2\beta_1$—known to regulate vacuole and lumen formation in collagen and fibrin gels.[29] Blocking $\alpha_2\beta_1$ integrin did not significantly reduce vacuole and lumen formation compared with the control (Figure 5A). However, blocking $\alpha_5\beta_1$ integrin reduced the extent of vacuole and lumen formation to 20%. Blocking $\alpha_v\beta_3$ significantly blocked vacuole and lumen formation to 10% after 48 hours. Moreover, we found α_v highly expressed on day 0, but this decreased during the culture period. We observed the up-regulation of α_5 on day 1 of culture, whereas the expression of both β_1 and β_3 decreased on days 2 and 3 of the culture period (supplemental Figure 5A). Because RGD peptides are primarily binding sites for α_v integrins, we examined whether the encapsulated ECFCs secrete fibronectin, which locally absorbs to the HA matrix and provides additional adjacent sites specific for α_5 integrin. Fibronectin was found to be up-regulated in encapsulated ECFCs. Moreover, confocal analysis detected deposition of fibronectin in the synthetic

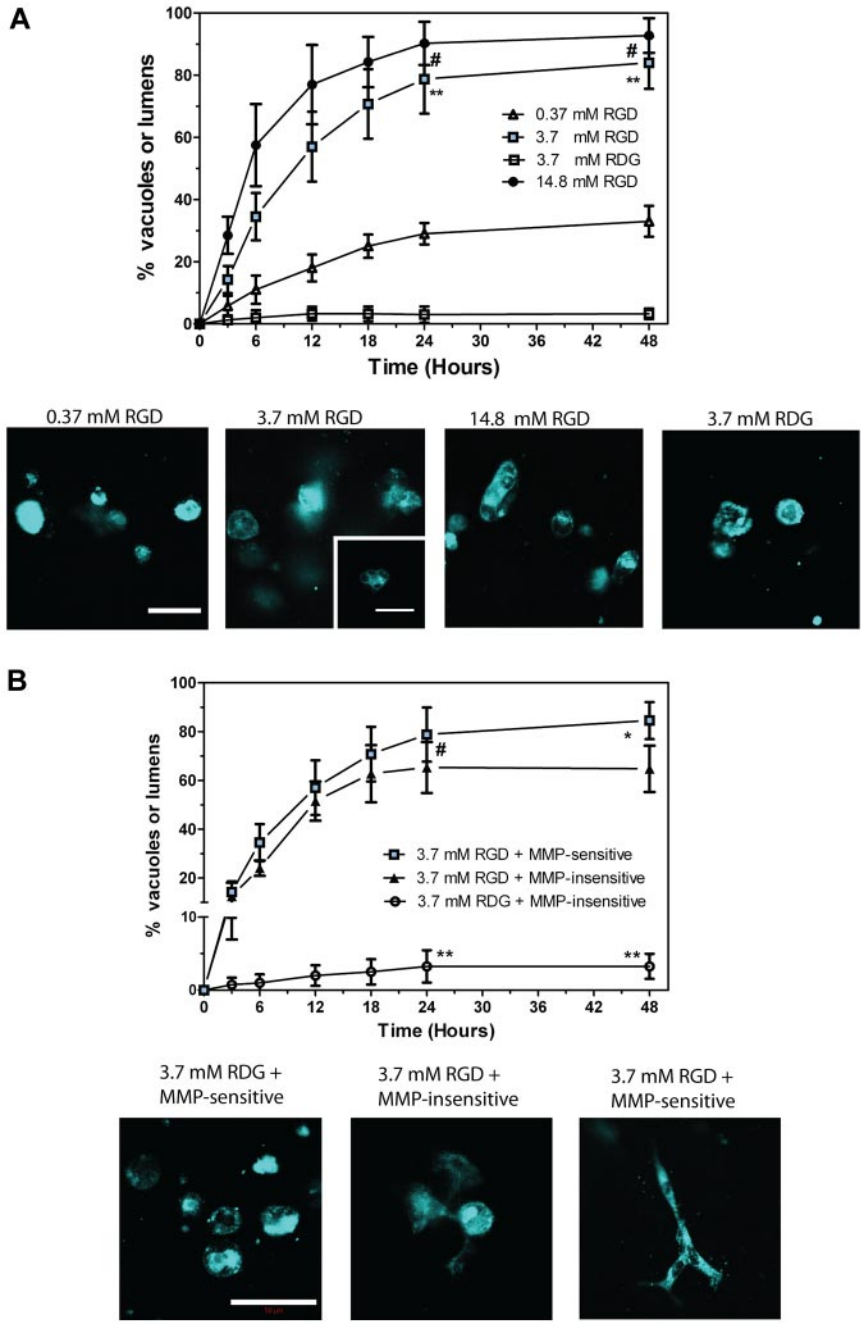

Figure 2. Matrix considerations. (A) RGD dose-dependent vacuolation of ECFC demonstrated by vacuole formation kinetics and represented images of vacuole vital stain FM 4-64 (cyan) at 24 hours. Scale bar is 100 μm. (Inset) High magnifications of single cells with abundant vacuoles in 3.7mM RGD. Scale bar is 20 μm. (B) Requisite of both RGD adhesion sites and MMP-degradable crosslinker for vacuolation of ECFC demonstrated by vacuole formation kinetics and represented images of vacuole vital stain FM 4-64 (cyan) at 24 hours. Significance levels were set at: $\#P > .05$, $*P < .05$, and $**P < .01$. Scale bar is 50 μm.

matrix. We suggest that new ECM deposited by the encapsulated ECFCs provides additional adjacent sites to provide specificity for α_5 integrin (Figure 5B; supplemental Figure 5B). Both MMP-1 and MMP-2 were localized near the cell membrane at day 2, when branching and sprouting started to occur (Figure 5C; supplemental Figure 5C).

Cell and material interactions: kinetics of matrix remodeling during vascular morphogenesis

We also characterized the dynamic interactions between ECFCs and HA hydrogels. We found that HA hydrogel stiffness decreased as vascular network formation progressed, reaching a low of 40 Pa, which agreed well with our previously published data (Figure 6A; supplemental Figure 6). However, gels that did not contain cells showed no significant reduction in mechanics on the same time-scale. To further investigate cellular remodeling of HA hydrogels by ECFCs, scanning electron microscopy analysis was performed. On day 1, we found rounded cells within the complex and dense hydrogel mesh. By day 3, the cells were primarily spread and formed multicellular networks between large guidance microchannels (supplemental Figure 7A). The vascular guidance microchannels formed within AHA hydrogels are clearly observed in scanning electron microscopy analysis performed on constructs without the cell-fixation step (supplemental Figure 7B).

EC migration through vascular guidance tunnels within collagen gels, which has proven to be MT1-MMP–dependent, enables the formation of complex lumen structures.[37,38] Correlating well with the progress in vascular guidance tunnel formation, we found that the expression of MMPs and hyaluronidases by the encapsulated ECFCs increased along the 3-day culture period. As vascular

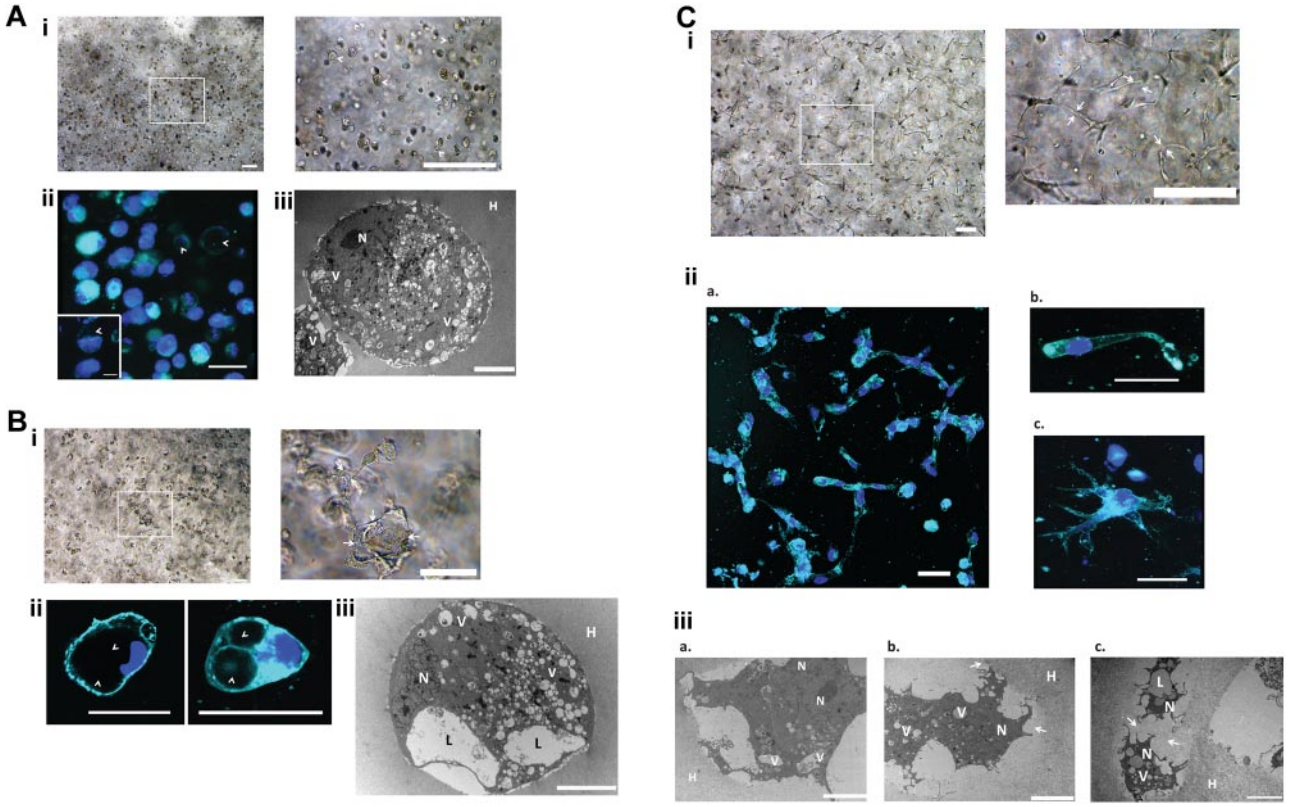

Figure 3. ECFC encapsulation, morphogenesis, and network formation in HA gels (days 0-2). A. Vacuole formation observed a few hours after cell encapsulation using: (i) Light microscopy (LM) imaging (left panel) and higher magnification of vacuolated cells (indicated by arrowheads; right panel); (ii) vacuole vital stain FM 4-64 (cyan; nuclei in blue) of encapsulated cells and higher magnification of a vacuolated cell (indicated by arrowheads; inset). Scale bars are 100 μm. (iii) TEM high-resolution representative image of a single, rounded encapsulated cell. Scale bar is 10 μm. (B) Increased number and size of vacuoles and merging into large lumen detected by day 1 of culture, as indicated by: (i) LM imaging (left panel) and higher magnification showing merging lumen (indicated by the arrows; right panel); (ii) vacuole vital stain FM 4-64 (cyan; nuclei in blue) high magnification focused on cells containing large vacuoles (indicated by the arrowhead; scale bars are 50 μm); and (iii) TEM high-resolution representative image of an encapsulated cell with apparent vacuoles. N indicates nucleus; V, vacuoles; L, lumen; and H, hydrogels. Scale bar is 20 μm. (C) Progression in tubulogenesis through branching and sprouting and hydrogel degradation observed using: (i) LM imaging of encapsulated cells on day 2 (left panel) and higher magnification focusing on branching networks (arrows indicate an example; right panel; scale bars are 100 μm); (ii) vacuole vital stain FM 4-64 (cyan; nuclei in blue) on day 2 illustrating representative images of (a) network formation, (b) branching cell, and (c) sprouting cell (scale bars are 50 μm); and (iii) TEM high-resolution representative images of: (a) a cell with degraded surroundings; (b) elongated cell morphology; and (c) guiding channels of degraded hydrogel formed between adjacent cells (indicated by arrows). N indicates nucleus; V, vacuoles; L, lumen; and H, hydrogel. Scale bars are 20 μm.

morphogenesis progresses, ECFCs express Hyal-2 and Hyal-3, as well as MT1-MMP, allowing the localization activity of secreted MMP-1 and -2 (Figure 6Bi). At the end of day 3, vascular networks formed within HA hydrogels stabilized, as evidenced by the increased expression of TIMP-1, TIMP-2, and TIMP-3 by ECFCs (Figure 6Bii).

Moreover, the progression in cellular remodeling of the HA hydrogels was observed at various points throughout vascular morphogenesis by monitoring the release of uronic acid, a byproduct of AHA degradation, and the encapsulated VEGF. During the culture period, AHA hydrogels gradually degraded and released the uronic acid by-product into the culture media (supplemental Figure 7Ci). As the hydrogels degraded, ~ 80% of the encapsulated VEGF was released into the media, providing a soluble cue for the ECFCs to undergo tubulogenesis (supplemental Figure 7Cii).

To further delineate whether MT1-MMP or other MMPs such as MMP-1 or MMP-2 are involved in this process, inhibition studies via TIMPs were performed. We found that the presence of TIMP-1 allowed vacuole formation and coalescence into an open lumen compartment but with limited network formation. In contrast, the presence of TIMP-2 or TIMP-3 allowed vacuole formation but not coalescence into an open lumen compartment and network formation, blocking the process of tubulogenesis, as it did to the negative control where GM6001 was added (Figure 6C). Hence, we concluded that in our synthetic matrix system, MT1-MMP, MMP-1, and MMP-2 are required for ECFC morphogenesis.

We were also interested whether Hyal-2 and/or Hyal-3 are directly involved in ECFC morphogenesis in the HA hydrogels. As mentioned in "Matrix considerations for vascular morphogenesis adhesion and degradation", vacuole formation occurred but did not progress to network formation when ECFCs were encapsulated in HA hydrogels made of a scrambled MMP-insensitive crosslinker (rather than MMP-sensitive crosslinker; Figure 2B). In addition, we performed siRNA suppression studies of MT1-MMP, Hyal-2, and Hyal-3. We found that when suppressing Hyal-2 and Hyal-3, vascular morphogenesis progressed comparable with the Luciferase-transfected cells. However, MT1-MMP–transfected cells formed vacuoles and some extent of branching without an open luminal structure (Figure 6D). We conclude that ECFCs encapsulated in our synthetic HA matrix undergo morphogenesis mainly through MMPs rather than hyaluronidases.

Functionality of ECFC vascular networks within AHA hydrogels

To determine the functionality of the engineered vascular networks, the 3-day matured and stabilized vascular constructs were subcutaneously implanted into nude mice. Histologic analysis revealed

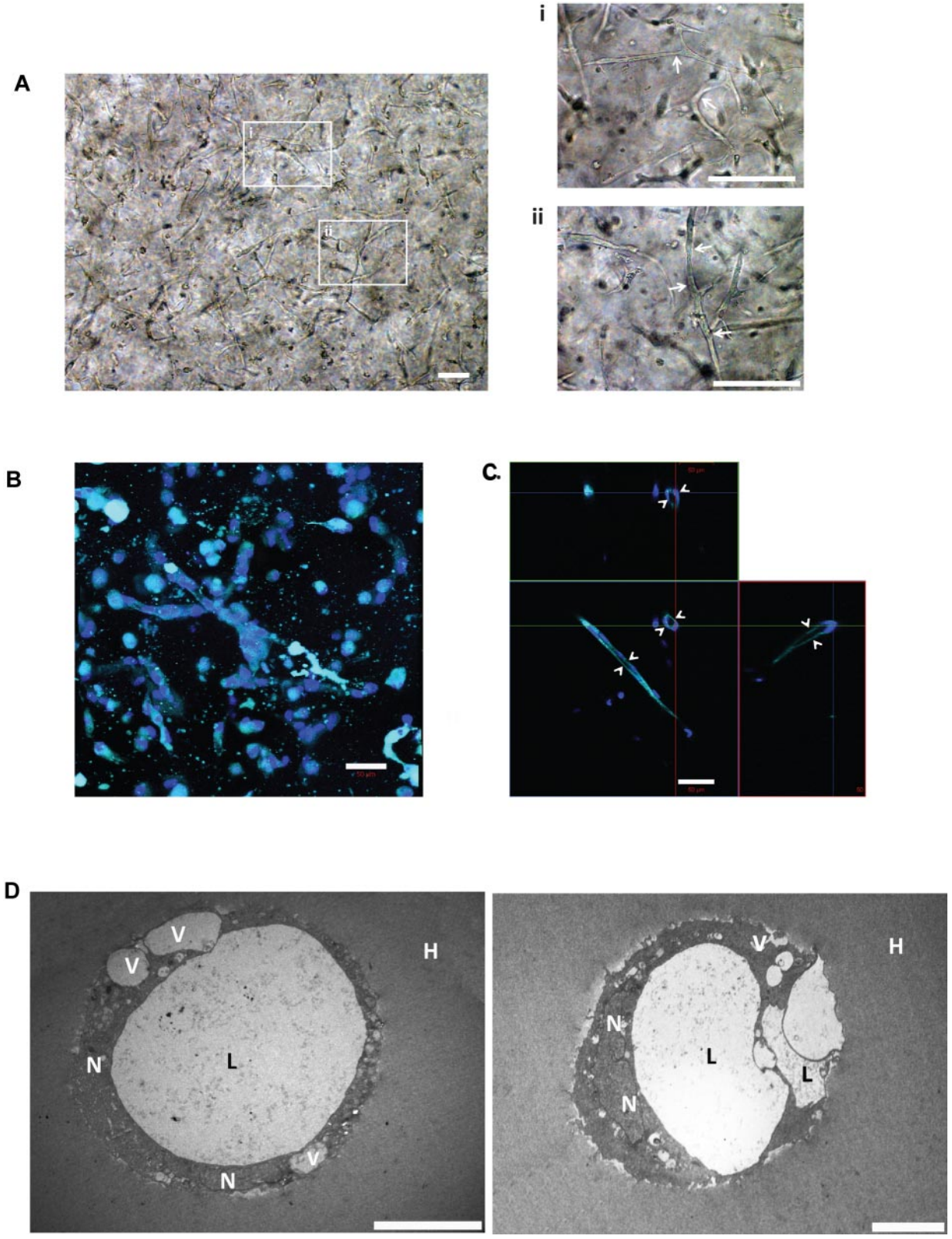

Figure 4. ECFC vascular network growth and complexity in HA hydrogels (day 3). (A) Left panel: Growth of comprehensive vascular networks are demonstrated using LM images at low magnification. Right panel: (i and ii) are high magnifications of white boxes (arrows indicate branched and elongated vascular networks). Scale bars are 100 μm. (B) Confocal analysis of vacuole vital stain FM 4-64 (cyan; nuclei in blue) demonstrating large lumen within the networks, and (C) demonstrated using orthogonal view (indicated by arrowhead). Scale bars are 50 μm. (D) TEM high-resolution images show cross-sections of matured vascular tube networks with enlarged lumens. Scale bars are 20 μm.

that the HA hydrogels degraded > 85% by 2 weeks postimplantation and that macrophages and tissue ingrowth replaced the degraded polymer (Figure 7A; supplemental Figure 8A). We observed host vasculature invading the periphery of the degraded hydrogel when implanting HA hydrogels both without or with ECFCs (supplemental Figure 8B-C; supplemental Figure 2A).

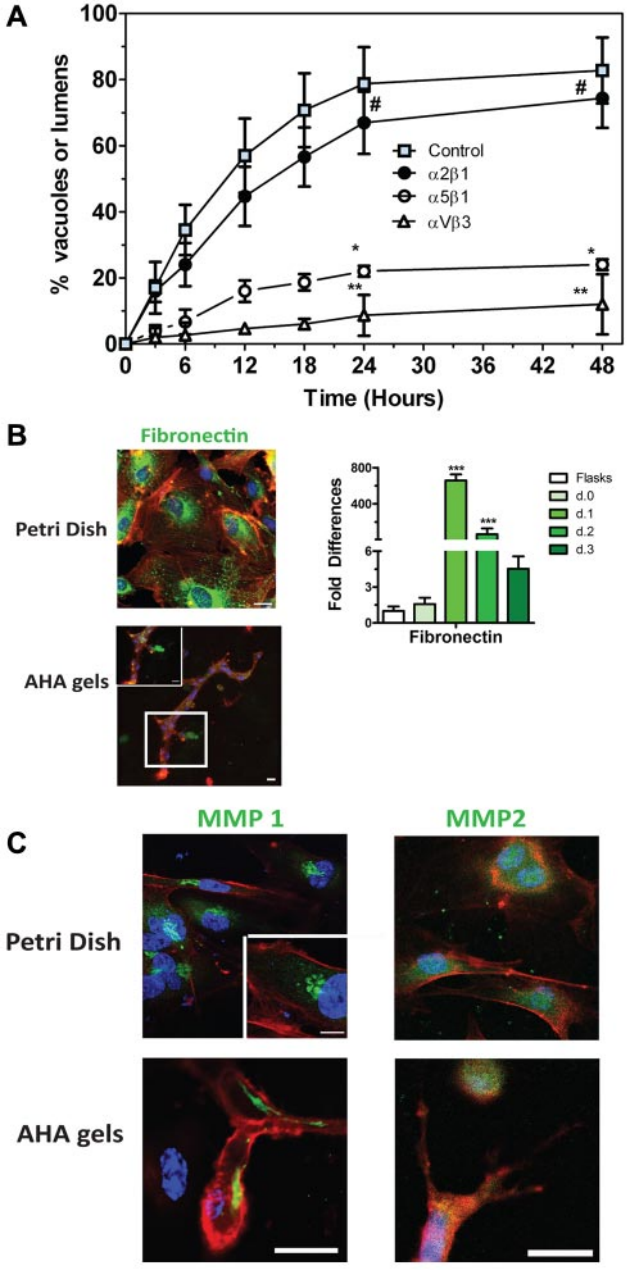

Figure 5. Cell and material interactions: adhesion. (A) Integrin-blocking assay revealed that RGD-dependent vacuolation and lumen formation within AHA hydrogels are regulated by $\alpha_V\beta_3$ and $\alpha_5\beta_1$ integrins, but not by $\alpha_2\beta_1$ integrins. (B) Real-time RT-PCR analysis reveals fibronectin expression of encapsulated ECFCs and confocal analysis detected some fibronectin deposited within the synthetic matrix (fibronectin in green; actin in red; nuclei in blue). (C) Confocal analysis revealed the membrane localization of MMP-1, and MMP-2 (both in green; actin in red; nuclei in blue) in the branching and sprouting ECFCs. Significance levels were set at: #$P > .05$, *$P < .05$, and **$P < .01$. Scale bars are 20 μm.

Such vasculature may help support the human vasculature growing within the hydrogel. When transplanting the human vascular constructs, we also observed microvessels (with cross-sectional areas ranging from 10 to 200 μm^2) that populated the center of the degraded hydrogels (supplemental Figure 8D). Such human microvasculature could not be detected in implants of HA hydrogels without ECFCs (supplemental Figure 8E). It is also important to note that the HA hydrogels without ECFCs are remodeled slower than the HA hydrogels encapsulated with ECFCs, as indicated by the presence of gel-mesh residues after 2 weeks (supplemental Figure 2A). We detected 2 types of microvessels at the center of the hydrogels: ~ 60% of the blood vessels contained both human ECFCs and host cells, while the remaining vessels contained only human ECFCs. Perfusion with blood cells could be detected in both types of microvasculature, demonstrating that the implanted ECFCs participate in the integration with the host vasculature and form functional human vascular networks that anastomose with the host vasculature to form functional vessels (vasculogenesis; Figure 7B-C; supplemental Figure 8F). Finally, we noticed that some microvessels perfused with blood cells and within the degraded HA hydrogel were positive for α-smooth muscle actin (Figure 7D), suggesting that host smooth muscle cells (SMCs) were recruited to microvasculature forming within the hydrogel transplant.

Discussion

The ECM contains the instructive physical and chemical cues required to delicately balance between various factors and cells to guide vascular assembly.[13,28,38,40,41] Depending on their spatial and temporal distribution throughout the body, each ECM component has a defined role in angiogenesis. HA and fibronectin, major components of the embryonic ECM, are vital vascular regulators during development.[22] In contrast, collagen and laminin, which are abundant in the adult ECM, are crucial for maintaining vascular homeostasis in adulthood.[42]

While natural ECM hydrogels have been widely used to study and deliver microvasculatures, synthetic materials offer the opportunity to control and modulate vascular morphogenesis and then deliver the engineered microvascular networks to in vivo environments. Although previous studies have used synthetic materials, such as self-assembling peptides[41] and PEG hydrogels,[20] to generate vascular networks in vitro, there is limited of translation in vivo. HA hydrogel is a synthetic biomaterial that can be tailored to create a modular culture system. Here, we demonstrate a highly controlled vascular morphogenesis and generate functional human vascular network formation in HA hydrogels.

Ingber and Folkman's pioneering study demonstrated that the concentration of fibronectin coating and EC seeding affects tubulogenesis on a 2-dimensional surface, establishing a link between the adhesion molecule presentation and vascular morphogenesis.[43] A recent study using fibrin gels specifically showed that RGD regulates vacuole and lumen formation in ECs, the first crucial step in vascular morphogenesis.[29] Previous studies optimized RGD concentrations in PEG hydrogels to enable fibroblast migration,[33,44] while a more recent study used fixed RGD concentrations to form networks of ECs in PEG hydrogels.[20] Using HA hydrogels, we have shown that RGD regulates vacuole and lumen formation in a dose-dependent manner and that an optimum concentration of RGD similar to that used in fibrin gels can enable vascular formation in synthetic hydrogels. Once vacuoles are formed, ECFCs migrate to their nearest neighbor to further coalesce into complex network structures. ECFC migration within 3-dimensional matrices requires an orchestrated balance between integrin activity, RGD ligand density, and proteolytic activity.[45] We found that an intermediate RGD density, which has been shown to allow optimal cell migration,[44] conduced to vascular morphogenesis and subsequent lumen formation and network branching. Indeed, studies of EC culture on surfaces coated with fibronectin corroborate these results; in these reports, the presentation of an appropriate RGD adhesion peptide resulted in EC retraction and the formation of branching capillary networks with hollow tubular structures.[43] MMP-sensitive peptide was also shown to be crucial in enabling network formation. Clearly, ECFC tubulogenesis in AHA gels requires both MMP-sensitivity and RGD peptides, presenting a novel opportunity for future studies decoupling

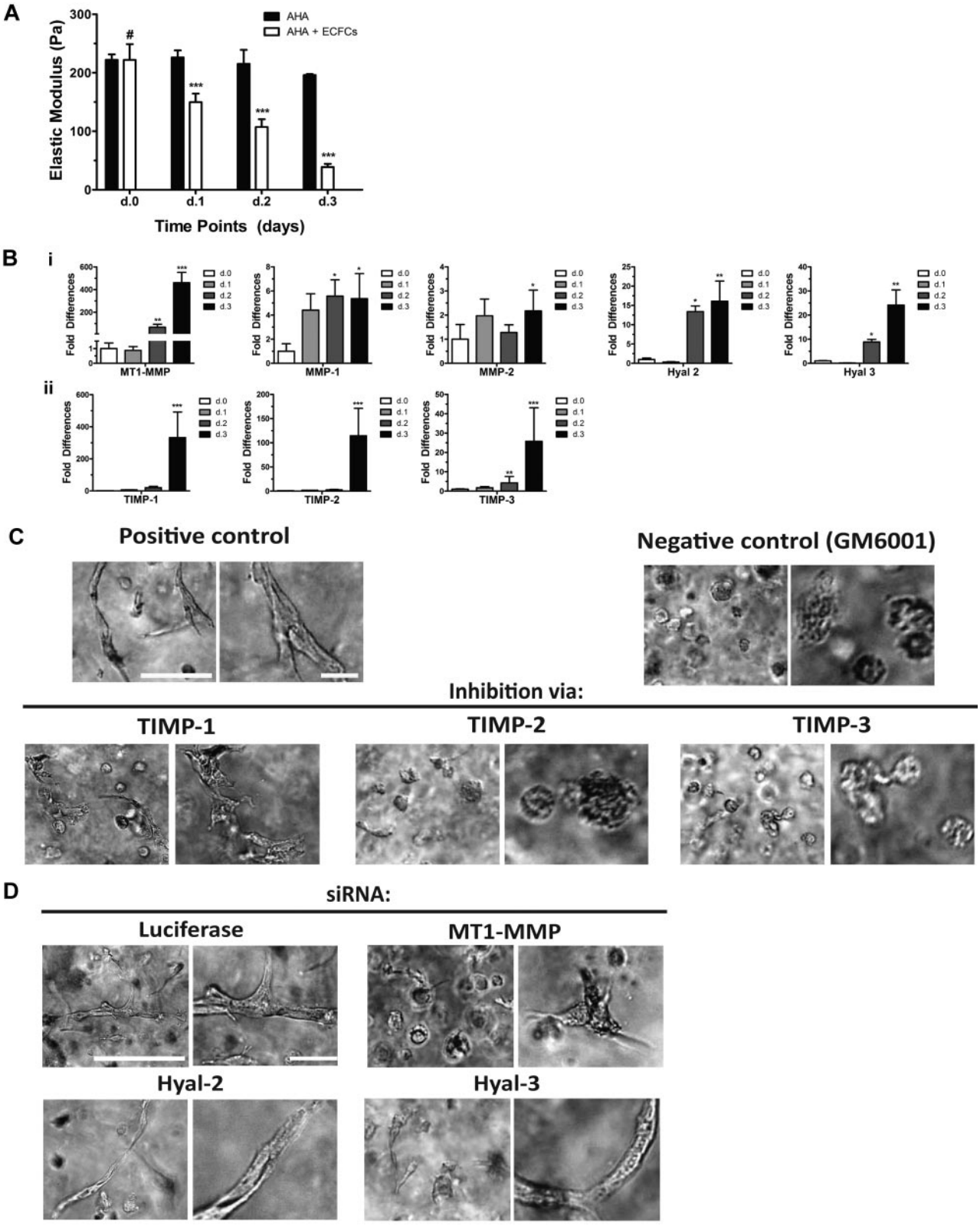

Figure 6. Cell and material interactions: matrix remodeling. (A) Viscoelasticity measurements revealed a decrease in hydrogel stiffness along the 3-day culture period, reaching 40 Pa in hydrogel encapsulated with ECFCs. (B) Real-time RT-PCR analysis shows increased expression of (i) MT1-MMP, MMP-1, MMP-2, Hyal 2, and Hyal 3 and (ii) TIMP-1, TIMP-2, TIMP-3, of encapsulated ECFCs along the 3-day culture period. Significance levels were set at: #$P > .05$, *$P < .05$, and **$P < .01$. (C) ECFCs undergo vascular morphogenesis in the absence (positive control) or presence of 5 μg/mL TIMP-1, TIMP-2, or TIMP-3. The presence of TIMP-1, TIMP-2, or TIMP-3 blocked tubulogenesis, as it did to the negative control (in the presence of 5μM GM6001). (D) siRNA suppression of MT1-MMP allowed vacuole formation and some extent of branching without luminal structures, while suppression of Hyal-2 or Hyal-3 did not affect vascular morphogenesis. Scale bars are 100 μm (left panel) and 10 μm (right panel).

those matrix parameters and analyzing their involvement in other signaling pathways during tubulogenesis.

Previous studies demonstrated that, within collagen and fibrin gels, vacuoles form a few hours after EC encapsulation, grow in

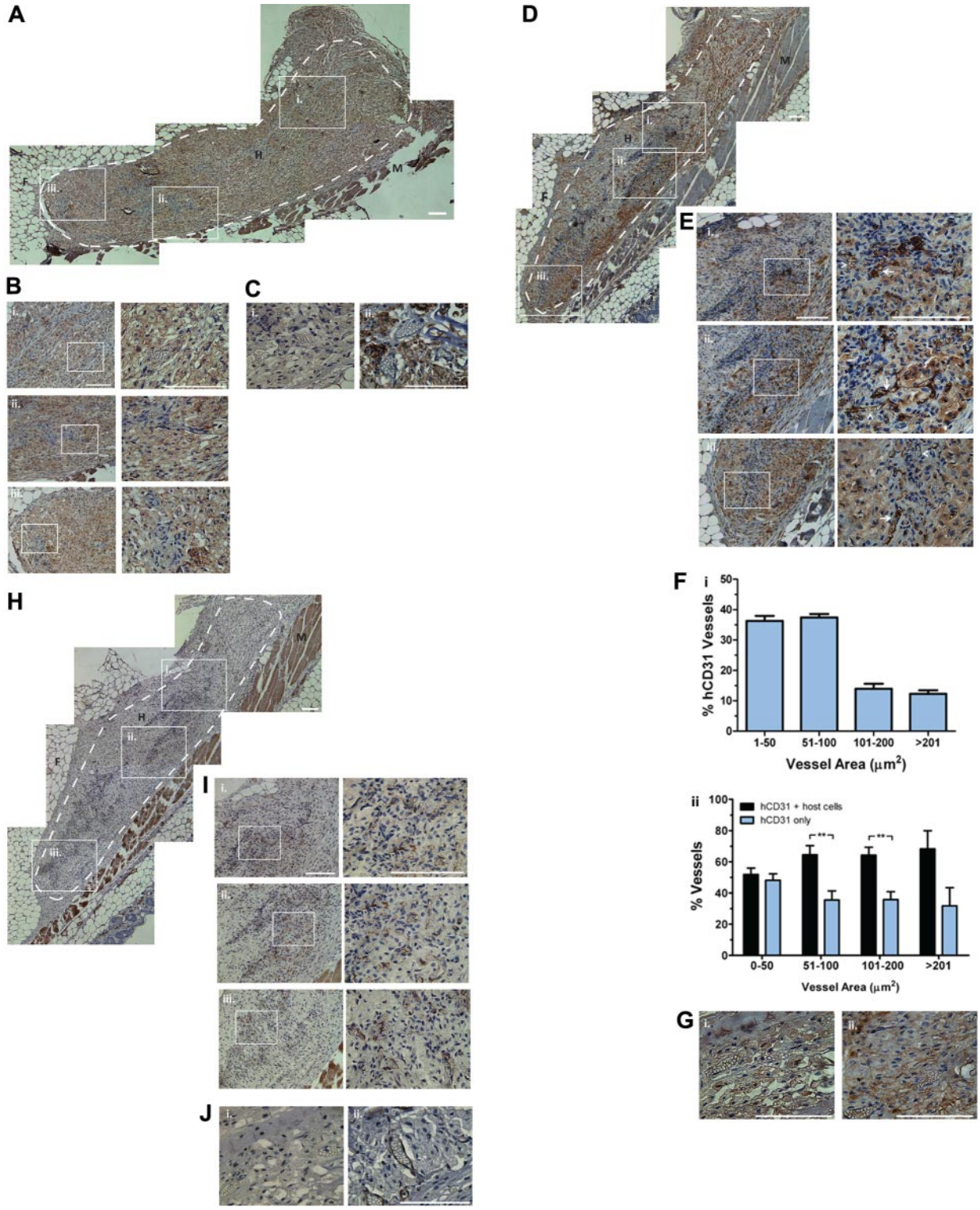

Figure 7. Functionality of vascular networks. (A) A montage of low magnification images of mouse F4/80-stained sections. (B) Subpanels i through iii are high magnifications of correlated boxes in panel A showing that macrophages degrade most implanted AHA hydrogels within 2 weeks of implantation, replacing them with macrophages (in brown) and tissue and vessel ingrowth (unstained cells). (C) Subpanel i, isotype control and subpanel ii, mouse F4/80-stained sections after 2 weeks of AHA only (without cells) implantation. (D) A montage of low-magnification images of human CD31-stained sections. (E) Subpanels i through iii are high magnifications of correlated boxes in panel D showing that ECFCs form microvessels with a human endothelial lining (some indicated by arrows), some of which contain blood cells and participate in the host angiogenesis, as indicated by the microvasculature containing both human ECFCs (some indicated by arrows) and unstained mouse host ECs (some indicated by arrowheads), which contain blood cells. (F) In subpanel i, quantification shows size distribution of microvessels with $CD31^+$ cells; in subpanel ii, quantification shows 40% of the vessels were solely human microvasculature, while the rest are vessels with both human ECFCs and host ECs. (G) Subpanel i indicates isotype control, and subpanel ii, human-CD31 -stained sections after 2 weeks of AHA only (without cells) implantation. Some microvessels found within the hydrogels, which contained blood cells, are positive for α-SMA, as demonstrated by panel H. A montage of low-magnification images of α-SMA–stained sections. (I) Subpanels i through iii are high magnifications of correlated boxes in panels H and J. (i) Isotype control; (ii) α-SMA–stained sections after 2 weeks of AHA only (without cells) implantation, suggesting that the vessels could recruit host SMCs to stabilize the engineered vessels. Significance levels were set at: $^*P < .05$ and $^{**}P < .01$. Dashed white lines indicate the periphery of the gels. H indicates hydrogels; M, muscle; and F, fat tissue. Scale bars are 100 μm.

size and quantities, and coalesce into lumen networks within 24 hours.[29] Using the AHA hydrogel system, we observed vacuoles within 3 to 6 hours after cell encapsulation progressively increasing in number and size until they coalesced into open lumen compartments by day 1. Specifically, in our synthetic culture system, integrin subunits α_5, α_V, β_1, and β_3 are highly expressed at this early stage of vascular morphogenesis (day 0 to day 1) to initiate vacuole and lumen formation through RGD-integrin signaling cascades. This phenomena was reported in fibrin gels[29] where RGD induced vacuole and lumen formation through $\alpha_5\beta_1$ and $\alpha_V\beta_3$, the main RGD-binding integrins.[46] More recently, β_1 integrin has been implicated to establish EC polarity and lumen formation.[47]

During the next stage of vascular morphogenesis, cells branch, sprout, and make connections with neighboring cells. To achieve this, cells use MT1-MMP to localize MMPs to the migratory end of the cell.[48] This local degradation allows cells to create "vascular guidance tunnels" and to migrate in a fashion similar to that observed within collagen gels.[37-38] In these synthetic gels, where peptides sensitive to MMP-1 and MMP-2 are used to crosslink the gels, we observed that sprouting and branching with open luminal structure requires mostly MMPs, such as MT1-MMP, MMP-1, MMP-2, but not Hyal activity. On the second day of AHA-ECFC construct culture, we observed tubulogenesis and cell elongation coupled with hydrogel degradation and guidance channel formation between neighboring cells. During this period, integrin expression was offset by an increase in MMP expression to support branching and network formation (day 2 to day 3). Overall, this data demonstrate that the synthetic material provides a responsive and dynamic niche to accommodate vascular morphogenesis by activating proteases specific to the tubulogenesis microenvironment.[17,37,38]

By day 3, TIMPs further stabilized complex luminal network structures. In collagen and fibrin gels, TIMPs expressed by ECs and pericytes were shown to stabilize mature vascular networks by inhibiting MMP activity.[30] This data suggest that prospective studies aimed at investigating in vitro long-term vasculature stabilization within hydrogels may require the incorporation of pericytes or SMCs.[49]

The importance of cellular remodeling during vascular morphogenesis has been reported.[13,26,41,50] The observed AHA hydrogel degradation, decrease in stiffness, evidence of vascular guidance tunnel formation, and increased expression of MMPs and hyaluronidases by the encapsulated ECFCs all agreed well with the progression of vascular morphogenesis. These trends highlight the novelty of our modular synthetic system in enabling dynamic interactions between material and cells during each stage of tubulogenesis.

Once implanted in vivo, macrophages were evident to quickly degrade the AHA hydrogels, allowing host tissues and vessels to invade and support the engineered microvascularized construct. This process let the human microvascular networks survive transplantation and rapidly anastomose with the host vasculature. Most microvessels were perfused with RBCs and contained both human ECFCs and host ECs, suggesting that the engineered human microvasculature anastomosed with the host vessels. Moreover, host SMCs, observed within the degraded AHA area, enabled the stabilization of the newly formed microvessels. As reported in other systems,[8,9,16,49] these data also suggest that future incorporation of pericytes or SMCs should be investigated to generate stabilized and long-lasting vessels.

Acknowledgments

The authors thank Dr Michael McCaffery from the Integrated Imaging Center at Johns Hopkins University (JHU) for TEM processing and imaging; Kyle Wong from JHU for assisting with Western blot and RT-PCR; and Dr Jennifer Elisseeff and Jeannine Coburn from JHU for assisting with microrheology measurements.

This research was partially funded by an AHA-Scientist Development grant and March of Dimes Basil O'Connor Starter Scholar Award (S.G.) and by National Institutes of Health grant U54CA143868.

Authorship

Contribution: D.H.-P. designed and performed research, analyzed data, and wrote the paper; V.B., Y.-I.S. and J.Y. performed research and analyzed data; K.F.-T. and C.S. analyzed in vivo data and helped edit the paper; S.K. and J.A.B. contributed new reagents, analyzed hydrogel data, and wrote the paper; and S.G. designed research, analyzed data, and wrote the paper.

Conflict-of-interest disclosure: The authors declare no competing financial interests.

Correspondence: Sharon Gerecht, Department of Chemical and Biomolecular Engineering, Johns Hopkins Physical Sciences-Oncology Center and Institute for NanoBioTechnology, Johns Hopkins University, 3400 N Charles St, Baltimore, MD 21218; e-mail: gerecht@jhu.edu.

References

1. Nor JE, Peters MC, Christensen JB, et al. Engineering and characterization of functional human microvessels in immunodeficient mice. *Lab Invest.* 2001;81(4):453-463.
2. Asahara T, Murohara T, Sullivan A, et al. Isolation of putative progenitor endothelial cells for angiogenesis. *Science.* 1997;275(5302):964-967.
3. Urbich C, Dimmeler S. Endothelial progenitor cells: characterization and role in vascular biology. *Circ Res.* 2004;95(4):343-353.
4. Silva EA, Kim E-S, Kong HJ, Mooney DJ. Material-based deployment enhances efficacy of endothelial progenitor cells. *Proc Natl Acad Sci U S A.* 2008; 105(38):14347-14352.
5. Schatteman GC, Hanlon HD, Jiao C, Dodds SG, Christy BA. Blood-derived angioblasts accelerate blood-flow restoration in diabetic mice. *J Clin Invest.* 2000;106(4):571-578.
6. Rafii S, Lyden D. Therapeutic stem and progenitor cell transplantation for organ vascularization and regeneration. *Nat Med.* 2003;9(6):702-712.
7. Shepherd BR, Enis DR, Wang F, Suarez Y, Pober JS, Schechner JS. Vascularization and engraftment of a human skin substitute using circulating progenitor cell-derived endothelial cells. *FASEB J.* 2006;20(10): 1739-1741.
8. Melero-Martin JM, De Obaldia ME, Kang SY, et al. Engineering robust and functional vascular networks in vivo with human adult and cord blood-derived progenitor cells. *Circ Res.* 2008; 103(2):194-202.
9. Au P, Daheron LM, Duda DG, et al. Differential in vivo potential of endothelial progenitor cells from human umbilical cord blood and adult peripheral blood to form functional long-lasting vessels. *Blood.* 2008;111(3):1302-1305.
10. Hirschi KK, Ingram DA, Yoder MC. Assessing identity, phenotype, and fate of endothelial progenitor cells. *Arterioscler Thromb Vasc Biol.* 2008;28(9):1584-1595.
11. Yoder MC, Mead LE, Prater D, et al. Redefining endothelial progenitor cells via clonal analysis and hematopoietic stem/progenitor cell principals. *Blood.* 2007;109(5):1801-1809.
12. Davis GE, Kon W, Stratman AN. Mechanisms controlling human endothelial lumen formation and tube assembly in three-dimensional extracellular matrices. *Birth Defects Res C Embryo Today.* 2007;81(4):270-285.
13. Kniazeva E, Putnam AJ. Endothelial cell traction and ECM density influence both capillary morphogenesis and maintenance in 3-D. *Am J Physiol Cell Physiol.* 2009;297(1):C179-C187.
14. Levenberg S, Rouwkema J, Macdonald M, et al. Engineering vascularized skeletal muscle tissue. *Nat Biotechnol.* 2005;23(7):879-884.
15. Critser PJ, Kreger ST, Voytik-Harbin SL, Yoder MC. Collagen matrix physical properties modulate endothelial colony forming cell-derived vessels in vivo. *Microvasc Res.* 2010;80(1):23-30.
16. Au P, Tam J, Fukumura D, Jain RK. Bone marrow derived mesenchymal stem cells facilitate engineering of long-lasting functional vasculature. *Blood.* 2008;111(9):4551-4558.
17. Lutolf MP, Hubbell JA. Synthetic biomaterials as instructive extracellular microenvironments for morphogenesis in tissue engineering. *Nat Biotechnol.* 2005;23(1):47-55.
18. Phelps EA, Landázuri N, Thulé PM, Taylor WR,

García AJ. Bioartificial matrices for therapeutic vascularization. *Proc Natl Acad Sci U S A.* 2010; 107(8):3323-3328.

19. Sieminski AL, Hebbel RP, Gooch KJ. The relative magnitudes of endothelial force generation and matrix stiffness modulate capillary morphogenesis in vitro. *Exp Cell Res.* 2004;297(2):574-584.
20. Moon JJ, Saik JE, Poche RA, et al. Biomimetic hydrogels with pro-angiogenic properties. *Biomaterials.* 2010;31(14):3840-3847.
21. Genasetti A, Vigetti D, Viola M, et al. Hyaluronan and human endothelial cell behavior. *Connect Tissue Res.* 2008;49(3):120-123.
22. Toole BP. Hyaluronan: from extracellular glue to pericellular cue. *Nat Rev Cancer.* 2004;4(7):528-539.
23. Vanderhooft JL, Alcoutlabi M, Magda JJ, Prestwich GD. Rheological properties of cross-linked hyaluronan-gelatin hydrogels for tissue engineering. *Macromol Biosci.* 2009;9(1):20-28.
24. Gerecht S, Burdick JA, Ferreira LS, Townsend SA, Langer R, Vunjak-Novakovic G. Hyaluronic acid hydrogel for controlled self-renewal and differentiation of human embryonic stem cells. *Proc Natl Acad Sci U S A.* 2007;104(27):11298-11303.
25. Hanjaya-Putra D, Yee J, Ceci D, Truitt R, Yee D, Gerecht S. Vascular endothelial growth factor and substrate mechanics regulate in vitro tubulogenesis of endothelial progenitor cells. *J Cell Mol Med.* 2010;14(10):2436-2447.
26. Yee D, Hanjaya-Putra D, Bose V, Luong E, Gerecht S. Hyaluronic acid hydrogels support cord-like structures from endothelial colony-forming cells. *Tissue Eng Part A.* 2011;17(9-10):1351-1361.
27. Khetan S, Katz JS, Burdick JA. Sequential crosslinking to control cellular spreading in 3-dimensional hydrogels. *Soft Matter.* 2009;5(8):1601-1606.
28. Mammoto A, Connor KM, Mammoto T, et al. A mechanosensitive transcriptional mechanism that controls angiogenesis. *Nature.* 2009;457(7233): 1103-1108.
29. Bayless KJ, Salazar R, Davis GE. RGD-dependent vacuolation and lumen formation observed during endothelial cell morphogenesis in three-dimensional fibrin matrices involves the alphavbeta3 and alpha5beta1 integrins. *Am J Pathol.* 2000;156(5): 1673-1683.
30. Saunders WB, Bohnsack BL, Faske JB, et al. Coregulation of vascular tube stabilization by endothelial cell TIMP-2 and pericyte TIMP-3. *J Cell Biol.* 2006;175(1):179-191.
31. Ismail JA, Poppa V, Kemper LE, et al. Immunohistologic labeling of murine endothelium. *Cardiovasc Pathol.* 2003;12(2):82-90.
32. Seliktar D, Zisch AH, Lutolf MP, Wrana JL, Hubbell JA. MMP-2 sensitive, VEGF-bearing bioactive hydrogels for promotion of vascular healing. *J Biomed Mater Res A.* 2004;68(4):704-716.
33. Raeber GP, Lutolf MP, Hubbell JA. Molecularly engineered PEG hydrogels: a novel model system for proteolytically mediated cell migration. *Biophys J.* 2005;89(2):1374-1388.
34. Augustin HG, Young Koh G, Thurston G, Alitalo K. Control of vascular morphogenesis and homeostasis through the angiopoietin-Tie system. *Nat Rev Mol Cell Biol.* 2009;10(3):165-177.
35. Chiu LLY, Radisic M. Scaffolds with covalently immobilized VEGF and Angiopoietin-1 for vascularization of engineered tissues. *Biomaterials.* 2010;31(2):226-241.
36. Han YP, Tuan TL, Wu H, Hughes M, Garner WL. TNF-alpha stimulates activation of pro-MMP2 in human skin through NF-(kappa)B mediated induction of MT1-MMP. *J Cell Sci.* 2001;114(1):131-139.
37. Stratman AN, Saunders WB, Sacharidou A, et al. Endothelial cell lumen and vascular guidance tunnel formation requires MT1-MMP-dependent proteolysis in 3-dimensional collagen matrices. *Blood.* 2009;114(2):237-247.
38. Sacharidou A, Koh W, Stratman AN, Mayo AM, Fisher KE, Davis GE. Endothelial lumen signaling complexes control 3D matrix-specific tubulogenesis through interdependent Cdc42- and MT1-MMP-mediated events. *Blood.* 2010;115(25): 5259-5269.
39. van Hinsbergh VW, Collen A, Koolwijk P. Role of fibrin matrix in angiogenesis. *Ann N Y Acad Sci.* 2001;936:426-437.
40. Deroanne CF, Lapiere CM, Nusgens BV. In vitro tubulogenesis of endothelial cells by relaxation of the coupling extracellular matrix-cytoskeleton. *Cardiovasc Res.* 2001;49(3):647-658.
41. Sieminski AL, Was AS, Kim G, Gong H, Kamm RD. The stiffness of three-dimensional ionic self-assembling peptide gels affects the extent of capillary-like network formation. *Cell Biochem Biophys.* 2007; 49(2):73-83.
42. Davis GE, Senger DR. Extracellular matrix mediates a molecular balance between vascular morphogenesis and regression. *Curr Opin Hematol.* 2008;15(3):197-203.
43. Ingber DE, Folkman J. Mechanochemical switching between growth and differentiation during fibroblast growth factor-stimulated angiogenesis in vitro: role of extracellular matrix. *J Cell Biol.* 1989; 109(1):317-330.
44. Gobin AS, West JL. Cell migration through defined, synthetic ECM analogues. *FASEB J.* 2002; 16(7):751-753.
45. Zaman MH, Trapani LM, Sieminski AL, et al. Migration of tumor cells in 3D matrices is governed by matrix stiffness along with cell-matrix adhesion and proteolysis. *Proc Natl Acad Sci.* 2006; 103(29):10889-10894.
46. Xu J, Rodriguez D, Petitclerc E, et al. Proteolytic exposure of a cryptic site within collagen type IV is required for angiogenesis and tumor growth in vivo. *J Cell Biol.* 2001;154(5):1069-1080.
47. Zovein AC, Luque A, Turlo KA, et al. beta1 integrin establishes endothelial cell polarity and arteriolar lumen formation via a par3-dependent mechanism. *Dev Cell.* 2010;18(1):39-51.
48. Chun TH, Sabeh F, Ota I, et al. MT1-MMP-dependent neovessel formation within the confines of the three-dimensional extracellular matrix. *J Cell Biol.* 2004;167(4):757-767.
49. Vo E, Hanjaya-Putra D, Zha Y, Kusuma S, Gerecht S. Smooth-muscle-like cells derived from human embryonic stem cells support and augment cord-like structures in vitro. *Stem Cell Rev.* 2010;6(2):237-247.
50. Stéphanou A, Meskaoui G, Vailhé B, Tracqui P. The rigidity in fibrin gels as a contributing factor to the dynamics of in vitro vascular cord formation. *Microvasc Res.* 2007;73(3):182-190.

2011 118: 804-815
doi:10.1182/blood-2010-12-327338 originally published online April 28, 2011

Controlled activation of morphogenesis to generate a functional human microvasculature in a synthetic matrix

Donny Hanjaya-Putra, Vivek Bose, Yu-I Shen, Jane Yee, Sudhir Khetan, Karen Fox-Talbot, Charles Steenbergen, Jason A. Burdick and Sharon Gerecht

Blood (print ISSN 0006-4971, online ISSN 1528-0020), is published weekly by the American Society of Hematology, 2021 L St, NW, Suite 900, Washington DC 20036.